FR9803461

I N2 P3
CENTRE D'ÉTUDES NUCLÉAIRES
DE BORDEAUX-GRADIGNAN
LE HAUT-VIGNEAU
33170 GRADIGNAN

CENBG 7818

Search for alpha particles emitted at rest in the break-up of the $^{12}C - \alpha - {}^{12}C$ molecule-like configuration

J.N. SCHEURER, D. BERTAULT; M. CAUSSAMEL , J.L. QUEBERT and J.P. FOUAN

K E Y W O R D S

E

NUCLEAR REACTION $^{12}C(^{16}O, ^{12}C^{12}C)\alpha$, measured $\sigma(E_1, E_2, \theta_1, \theta_2, E_{c.m.}(\alpha) = 0)$; $^{12}C(^{16}O, \alpha)$, measured $\sigma(\theta = 0, E_{c.m.}(\alpha) = 0)$. E = 40-65 MeV. Aligned configuration deduced.

SEARCH FOR ALPHA PARTICLES EMITTED AT REST IN THE BREAK-UP OF THE $^{12}C - \alpha - ^{12}C$ MOLECULE-LIKE CONFIGURATION

J.N. SCHEURER, D. BERTAULT, M. CAUSSANEL, J.L. QUEBERT

Centre d'Etudes Nucléaires de Bordeaux Gradignan
Institut National de Physique Nucléaire
et de Physique des Particules
Le Haut Vigneau 33170-GRADIGNAN-FRANCE

and

J.P. FOUAN
Centre d'Etudes Nucléaires de Saclay
Service de Physique Nucléaire à Basse Energie
B.P. n°2 ; 91190 GIF SUR YVETTE-FRANCE

ABSTRACT : A yield of alpha particles emitted at rest is clearly observed in $^{16}O + ^{12}C$ at several incident energies. These alpha particles are detected by two methods : i) the alpha particle is considered as a missing mass in the detection of two ^{12}C nuclei in coincidence ; ii) the alpha particle is detected at zero degree with a velocity due to the centre of mass motion. Such a yield is assigned to a linear chain formation of the type $^{12}C - \alpha - ^{12}C$ and an excitation function between 40 and 65 MeV is given. The emission due to Coulomb effects is emphasized in the discussion to give the chief explanation of the coincidence results.

1. THREE-BODY BREAK-UP AND PARTICLE EMITTED AT REST ; CHARACTERISTICS OF THE CONFIGURATION

High spin states found at high excitation energy in some light nuclei have been recently interpreted in the framework of molecule-like configurations [1] ; these states are studied by considering two subunits with their own intrinsic excitation, in a coupling scheme of the different angular momenta [2]. More complex configurations have also been examined in such a model, especially when three clusters are involved. Concerning the ^{28}Si case, which is considered here, the $^{12}C - \alpha - {}^{12}C$ structure has been studied according to its different degrees of freedom in linear [3, 4] and also triangular configurations [5].

In the present work we present experimental data which give a non negligible probability of the alignment of the three clusters for a state described as $\Psi = C_L$ (⟷) + C_T (△). Due to the non orthogonality of the two extreme solutions one can expect that $C_L \neq 0$. From a classical point of view, this means that, if the triangular configurations are a priori the most probable cases to consider, the linear chain with an α particle close to the centre of mass of the two ^{12}Cs may also be favoured.

The interest in such a structure was initially motivated [6] by the qualitative argument that only this molecule-like configuration is able to leave an experimental signature in the final stage of detection i.e. $^{12}C + \alpha + {}^{12}C$. For triangular cases, the Coulomb forces smear

out the initial configuration when the break-up takes place ; the linear case, on the contrary, gives rise to a specific emission of the α particle which remains at rest because of the compensation of the different forces. Such configurations are considered qualitatively in fig. 1, from a classical point of view. The initial configuration is a priori not known, since we have no knowledge of the wave function describing the state of the three clusters ; however, one can expect different qualitative features for the detection of aligned and non aligned configurations, namely, two types of emission should be favoured in the break-up : i) the α particle is emitted with a negligible energy in aligned configurations (even if angular momentum is given to the system) ; ii) the α particle is emitted with an energy ξ_α which results from its Coulomb trajectory in the case of slight unalignment or triangular configuration. This latter case is expected to give a specific recoil to the two ^{12}C nuclei, since the Coulomb forces should favour an average angle of emission relative to the ^{12}C - ^{12}C axis. Thus, the two ^{12}C nuclei are expected to recoil with roughly equal energies if the α particle is educed at 90 degrees.

Our experimental study was designed to look for evidence of such specific emissions, which are always characterized by two ^{12}C's emitted with equal, or roughly equal, c.m. energies. The ^{16}O + ^{12}C entrance channel was chosen to reach the excitation energy region where resonances have been observed in different exit channels [7-20].

The exit channel $^{12}C + \alpha + {}^{12}C$ was first studied for another purpose by Wieland et al[21], near 58 MeV. These authors who also studied other exit channels, concluded that, amongst the two final state in-

teractions which are expected, i.e. $^{16}O^{*}$ and $^{24}Mg^{*}$, the former is found to occur near 10 MeV in ^{16}O (probably the 4^{+} state at 10.34MeV) when the latter is not observed ; besides, the two-body channel $\alpha + {}^{24}Mg^{*}$ does not exhibit residual states higher than about 21 MeV, i.e. no α particles are detected with small energy.

In this study, we intend to show, through the search for aligned or quasi-aligned chains that the above results can be well explained by consideration of the initial structure. For instance, we qualitatively understand that a ^{24}Mg nucleus cannot be formed by fusion of two ^{12}C's if the third particle (α) prevents this process when lying in the vicinity of the centre of mass of the two heavy-core system. However, such alignments do not forbid the emission of α particles with small energies ; the only difference being that these α's of small energy are not related to ^{24}Mg states. In the same way, the final state interaction α - ^{12}C is more probable than ^{12}C - ^{12}C for such structures, explaining why the $^{16}O^{*}$ formation may be detected near the $^{12}C + \alpha$ threshold. In fact, we shall try to show in the last part of this work that the three-body Coulomb forces may also give an explanation of some coincidence results.

Besides the conclusion which can be drawn for such structures when an alpha particle is emitted at rest, a quantum effect is also expected because the energy $\varepsilon_{\alpha} = 0$ is only compatible with zero angular momentum : since the two undistinguishable ^{12}C's have a necessarily even angular momentun L_{12}, the total spin value $\vec{J} = \vec{L}_{12} + \vec{L}_{\alpha}$ has also to be even when $\varepsilon_{\alpha} = 0$. Thus, detection of such events gives a way to relate the intrinsic structure to definite even spin values.

2. EXPERIMENTAL EVIDENCE FOR ALPHA PARTICLES EMITTED AT REST

Two methods were used to detect such particles in the reaction $^{16}O + {}^{12}C \rightarrow {}^{12}C + \alpha + {}^{12}C$. The experiments were carried out at Saclay with 40 to 65 MeV ^{16}O beams from the FN Tandem Van de Graaff.

The first method consists in the detection of two ^{12}C's in coincidence, the α particle being a missing mass. Three-body kinematics is used to calculate the lab. angles ψ_1, ψ_2 at which two counter telescopes have to be set for the observation of such events.

The second method consists of direct detection of the α particles. This detection must be performed at zero degrees, in the beam direction, since all the postulated events will yield the α particles in this direction with lab. energies due to the centre of mass motion

$$(E_\alpha(0°) = \frac{m_\alpha m16_O E(^{16}O)}{(m^{16}O + m^{12}C)^2} \simeq 3 \text{ to } 5 \text{ MeV}).$$

This last method is certainly the best, since one obtains the total cross-section at once by counting the α particles of such energy. However, the technical difficulties of detection in presence of the beam (background filtering) make the first method useful as a necessary check for the existence of the proposed events. The zero degree detection was performed mainly by deflecting the α particles out of the beam and determining their $\frac{\Delta E}{E}$ and energy with a solid state counter telescope as shown in Fig. 2. A QDDD system was also used at some incident energies.

2.1. ^{12}C - ^{12}C COINCIDENCE EVENTS DUE TO SMALL α ENERGIES

The detection of two ^{12}C's in coincidence, corresponding to small α energies, must be carried out at specific angles. The calculation of such angles is straightforward when $\varepsilon_\alpha = 0$, since the emission is two-body-like, as shown in the insets of Fig. 7 and Fig. 8. Such emissions may be considered at different directions θ relative to the beam in the c.m. system. Fig. 3 shows the cases due to the choice of different directions (in the upper part, $\theta = \pi/2$). However, the three-body nature of the emission implies that other ^{12}C - ^{12}C events will also be detected at ψ_1, ψ_2 with other lab. energies E_1, E_2. These energies are given by the relation,

$$E_1(m_1 + m_3) + E_2(m_2 + m_3) + 2\sqrt{m_1 m_2 E_1 E_2} \cdot \cos\psi_{12} - 2\sqrt{A_1 m_1 E_\theta E_1} \cdot \cos\psi_1 - 2\sqrt{A_1 m_2 E_\theta E_2} \cdot \cos\psi_2 + A_1 E_\theta - m_3(Q + E_\theta) = 0.$$

E_θ is the incident energy in $A_1 + A_2 \rightarrow m_1 + m_2 + m_3 + Q$, ψ_{12} is the relative angle between the two detectors (coplanar detection in the experiment).

For any set of solutions, E_1, E_2, of the above equation, the relevant α energies in the c.m. system are usually different from zero except in (a) or (a'), shown in Fig. 3. Other points are shown in the same figure ; their population may be useful for spin assignments, since they correspond to some limiting cases in angular correlation studies (see discussion in 4.2.3).

2.1.1. Symmetric detection ; results between 45 and 50 MeV

The angle, θ, between the common direction of the momenta of the two ^{12}C's and the beam axis (angle which has no significance for non-aligned configurations) was chosen to be $\pi/2$ for this coincidence experiment.

The events of interest are expected in zone (a), as shown in the upper part of Fig. 3. The measurements were carried out in steps of 0.5 MeV between 45 and 50 MeV. The lab. angles were slightly corrected at each incident energy, to keep the value $\theta = \pi/2$.

Three plots showing the density of the coincidence events versus their respective lab. energies, E_1 and E_2, are shown in Fig. 4, 5 and 6.

The sorting of these events was obtained by gating the two particle identification and time spectra in order to select $^{12}C - ^{12}C$ true coincidences from the multiparameter recording of the events on tape. The target thickness was 200 $\mu g/cm^2$.

It is surprising to observe the accumulation of the coincidence events only in the zones (a) and (b) previously defined in fig. 3. In both cases, the events correspond to ^{12}C nuclei emitted with roughly equal energies (the small α energies however, correspond only to region (a)). At any incident energy, this feature (the accumulation in (a) and (b) only) is observed when other kinematically possibilities are open along each locus between (a) and (b). The width of the distribution is due to the finite apertures of the coincidence detectors which cover some range of c.m. geometries.

The events searched for are clearly present in region (a), and the corresponding α energies may be determined for different slices of this area ; they correspond to a range $0 \leq E_\alpha \leq 900$ kev.

In some cases as in fig. 5 (48 MeV) the area $0 \leq E_\alpha \leq 50$ kev is not fed at all and this is to be related to the spin effects mentionned earlier, which might forbid this region if the total angular momentum, J, is odd.

2.1.2. Results obtained with assymmetric detection at 46 MeV

The energy of 46 MeV was chosen in the early stages of the experiments to excite the well known 19.7 MeV resonance. In fact, the low coincidence rate obtained required the use of a 300 $\mu g/cm^2$ ^{12}C target. The actual incident energies thus ranged between 43 and 46 MeV and the results described here may not be directly comparable to those obtained at 46 MeV in other exit channel

Measurements were performed for the following θ values (defined in Fig. 3) : 99, 104, 112, 126, 136 and 142 degrees. Two of the coincidence diagrams obtained are shown in Figs. 7 and 8. In these cases, if some events related to very small α energies (100 keV) are recorded, the area defining the strict zero energy is not dominantly fed. This result may be related to the spin of the system which, in this case, should be odd. This situation makes the comparison with the 19.7 MeV resonance difficult since its J value is usually given to be even (14^+). Again, the events which are scattered on the left side of the diagram in Fig. 7 correspond to ^{12}C nuclei emitted with roughly equal c.m. energies, but, in this case, the α c.m. energies are no longer very small (1.4 to 3 MeV).

2.2. ALPHA PARTICLES DETECTED AT ZERO DEGREES

Zero-angle detection allows the observation of particles of small energies $\mathcal{E}_\alpha$, emitted in backward and forward directions in the c.m. system.

The corresponding Lab. energies are :

$$(u^{1/2} - \mathcal{E}_\alpha^{1/2})^2 \leq E_\alpha(0°) \leq (\mathcal{E}_\alpha^{1/2} + u^{1/2})^2$$

with $u = \dfrac{m_\alpha m^{16}0\ E(^{16}0)}{(m^{16}0 + m^{12}C)^2} > \mathcal{E}_\alpha$

When $\mathcal{E}_\alpha = 0$, the recorded events correspond to all the θ values defined in 2.1 for the ^{12}C - ^{12}C relative emission. This is a way of directly recording the integrated cross section for such events.

The sensitivity to the α c.m. energies is high : for instance, the α events with c.m. energies $0 \leq \mathcal{E}_\alpha \leq 150$ keV are scattered in the range of 2.9 to 6.3 MeV in the Lab. system at 53 MeV. Such detection requires the use of a deflection system. An electrostatic separator and, in some cases, a QDDD spectrometer were used.

In both experiments, it is necessary to damp the background of spurious events coming from different charge states in the beam. The events are selected in q/E by the electrostatic deflector. It is then necessary to eliminate the low energy tails of the beam, due to parasitic slit scattering. This was achieved with the beam transport system consisting of two quadrupole doublet lenses with a slit system,

set at the intermediate image, and appropriate beam steerers. All other collimators were removed from the beam path (i.e. before the ^{12}C target as well as at the deflector entrance). The counter telescope was set at 4 cm from the undeviated beam axis (see Fig. 2). Its collimation system was designed to look fully at the central part of the deflector plates, in order to get as a large an acceptance in energy as was compatible with the required beam suppression. This energy acceptance was estimated to be 3 MeV, meaning that the detection efficiency is approximately constant for alpha energies equal to E°_{α} ($\xi_{\alpha} = 0$) $\pm$ 1.5 MeV with the appropriate voltage setting on the deflector plates. Typical energy spectra gated by the alpha particles E $\times \Delta$E identification are shown in Figs. 9 and 10.

Another set of measurements was performed with a QDDD at zero degree. The incident beam was stopped by a tantalum plate situated in the first dipole. The interesting α energies were easily selected, since the ratio of their magnetic rigidity, compared to that of the beam, is :

$$B\rho\ (\text{beam})/B\rho\ (\alpha) = \frac{1}{2}\ (A_1 + A_2)\ /\ (m_{\alpha} A_1)^{1/2} = 1.75$$

where A_1, A_2 stand for ^{16}O and ^{12}C masses respectively. The α particles were further identified by their ΔE signal in a thin position gas counter. . The relevant energy spectrum was studied between 2 and 7 MeV by changing the field value and monitoring each run by complementary Rutherford scattering of the ^{16}O beam at 30° lab. For this purpose, a gold layer ($1\mu g/cm^2$) deposited onto the target ($30\mu g/cm^2$) was used. Fig. 11 shows a typical α spectrum obtained by such a method at 53 MeV incident energy.

It can be seen in Figs. 9 to 11 that at some incident energies, a peak is clearly observed right inside the range of the expected zero α energies (c.m.). An excitation function of such events between 40 and 65 MeV is shown in Fig. 14. The continuum background, which is best seen in Fig. 11 at high energy (because this part is not damped as in the telescope method), is attributed to kinematic compensations which can yield parasite events, as discussed below.

Indeed, it is necessary to discuss this point in detail. Since no coincidences were used in this method, we expect a selectivity of the events only by picking up a specific direction (0°) and a particular energy (c.m. motion). We therefore have to consider all the processes which could yield α particles with the same Lab. energy. Several possibilities are mentionned below:

$^{16}O + {}^{12}C \longrightarrow$ (1) $\alpha + {}^{24}Mg^{*}$ or $\alpha + {}^{24}Mg^{*} \hookrightarrow {}^{12}C + {}^{12}C$

(2) ${}^{20}Ne^{*} + {}^{8}Be \hookrightarrow 2\underline{\alpha}$

(3) ${}^{12}C^{*} + {}^{16}O^{*} \hookrightarrow \underline{\alpha} + {}^{12}C^{*}$

(4) ${}^{12}C + {}^{16}O^{*} \hookrightarrow \underline{\alpha} + {}^{12}C^{*}$

(5) $\alpha + {}^{24}Mg^{*} \hookrightarrow \underline{\alpha} + {}^{20}Ne^{*}$

The starred species are excited and the underlined α's are those which would be detectable.

The three-body emission of the first case can be considered to be a two-body process, since the particle is emitted in the first step of the sequential decay. We assign to this case events which do not yield a second α particle (e.g., $^{24}Mg^{*} \longrightarrow {}^{12}C + {}^{12}C$). It is clear that such a process may give α Lab. energies lower and higher than the mean value expected $(\mathcal{E}_{\alpha} = 0)$. It is also obvious that an α emission with $\mathcal{E}_{\alpha} = 0$ is impossible in a two-body process, because of recoil effects and Coulomb barrier considerations. Furthermore, the α energies corresponding to the left or the right of the observed peak are deduced to be very small ($\mathcal{E}_{\alpha} \ll u$). They would correspond to completly excited ^{24}Mg and would be damped for the same reasons (an α c.m. energy of at least a few MeV is required to go through the $\alpha + {}^{24}Mg$ Coulomb barrier).

The possibility of parasite events are more serious with the other cases, which yield an α particle in the second step. In such cases, the α particle may have its velocity in a direction opposite to that of the recoiling intermediate nucleus. Thus, its net c.m. energy may be zero and its laboratory velocity might correspond to that expected for alpha particles emitted at rest. The following comments suggest that this is very unlikely to occur:

Kinematic calculations for cases (2) to (5) were performed in order to select the virtual levels which could be involved to yield α particles with equivalent $\mathcal{E}_{\alpha} \simeq 0$. The second and third reactions can easily be ruled out by kinematics. The only remaining candidates are found to be the last two processes (see Fig. 12) with the following values :

levels in $^{16}O^*$ at $E^* = 8.5$ to 9 MeV

levels in $^{24}Mg^*$ at $E^* = 9.8$ to 10 MeV

This leads to the following conclusions :

i) the values of the excitation energies found for such possible "states" do not correspond to existing states which are good α emitters. Moreover, these values are very close to the $\alpha + {}^{12}C$ and $\alpha + {}^{20}Ne$ thresholds respectively. This means that the available energy of the α particle in such systems would be very small and incompatible with Coulomb barrier considerations : the α particle would thus be expected to be trapped rather than reemitted. An exception to this Coulomb barrier effect can occur when the three clusters are aligned. Then, the cluster not involved in the two-body interaction (e.g., the first ^{12}C in the 4th case) could lower the barrier. This remark brings us back to our initial considerations on aligned chains. It is then difficult to consider that the $\varepsilon_\alpha = 0$ emission is the conventional final-state interaction.

ii) The two-body final state interaction is of second order in intensity since only particular directions (close to π) of the α velocity in the recoiling intermediate nucleus system will contribute in our range of energies.

iii) A compensation of two opposite velocities to give a net result corresponding to a virtual zero energy in the c.m. system is only valid at one incident energy. A splitting occurs versus this incident energy (see the straight lines in fig. 12), and this is not observed experimentally.

This discussion demonstrates, once more, that usual final state interactions are difficult to consider in terms of aligned clusters for which the Coulomb barriers are strongly enough perturbed to allow free emission of a particle or an exchange of cluster from one centre to the other. The α spectra obtained at zero degrees are thus necessarily due to linear configurations of the three clusters in which the α particle is right at the centre of symmetry of the chain (case where $\varepsilon_\alpha = 0$; see the spectrum at 53 MeV) or very slightly off-center with regard to the axis r_{12} ($\varepsilon_\alpha \simeq 50$ kev). This is clearly seen in the α spectra for which, in some cases, the small α energies ($\simeq 50$ kev) seem to be favoured compared with strictly zero energy. This result may be considered from another point of view, namely, taking into account the quantum effects which forbid this region, $\varepsilon_\alpha = 0$, for odd J value.

3. CROSS SECTIONS

The coincidence results correspond to differential cross sections, while zero degree detection gives access to the total cross-section.

The integration of events in the region of negligible α energy corresponds to symmetric or almost symmetric aligned structures. However, as already mentioned, quantum effects can be seen in regions of very small α energies. This is illustrated at 48 MeV by the coincidence plot or at 45.5 and 49 MeV in the α spectra obtained at zero degree. The definition of such areas in the different spectra is thus rather delicate. The excitation functions relative to coincidence events falling in region (a) and (b) are shown in fig. 13. More accurate integrations may be performed on different slices of α energies in (a). This is shown for $0 < E_\alpha < 50$ kev in Fig. 14, where these coincidence results and the results of detection at zero degrees have been plotted together.

Such an excitation function suggests that a resonance occurs at about 45.5 MeV (19.5 MeV c.m.) corresponding certainly to an even spin value. But on both sides of the resonance the spin value is certainly odd. A strong yield is also observed in the 52-65 MeV region (22-28 MeV c.m.) where resonant behaviour is more difficult to define. This region, according to our hypothesis, is strongly related to structures with even spin values and aligned configurations. Identification of the 45.5 MeV resonance found by this method, with the well known resonance at 46 MeV does not seem to hold because of the shift in energy and

the small probability of coupling this resonance to the exit channel studied here [2].)

In general, no relation is evident between the present results and those obtained for elastic and inelastic channels. For example, at 22 MeV (c.m.) Shapira et al[20]) find a J value of 15^-, whereas our results, due to the selectivity of the events, are in favour of an even spin value.

4. DISCUSSION AND INTERPRETATION OF THE RESULTS

4.1. EXCITATION FUNCTION

The aligned configuration is chiefly observed in the region of 50 to 65 MeV. An extrapolation of the behaviour of the excitation function towards lower energies gives a threshold at about 40 MeV. The excitation energy corresponding to this threshold lies 10 MeV above the Q value of the $^{12}C + \alpha + {}^{12}C$ configuration. This result is in agreement with a simple calculation of the total Coulomb potential for a linear chain

$$Vc = 1.44\ Z_1 \left[Z_2 + 4Z_3 \right] \ / \ r_{12}$$

where r_{12} is the size of the chain and has to be greater than, or equal, to the sum of the nuclear radii; i.e. $r_{12} \gg 2\ r_0\ (m_{^{12}C}{}^{1/3} + m_{\alpha}{}^{1/3})$ which, in turn, yields the value $r_0 = 1.56$ fm

The resonant behaviour of the production of α particles at rest is much less clear. In the upper part of Fig. 14 we have indicated the level positions calculated for a rigid linear chain [3]) and no obvious relationship with such rotational states appears in the cross section behaviour as a function of incident energy.

It is worth noting that Wiebicke et al [5]) predict triangular shapes, rather than linear ones, to exist at lower energies. This statement seems to be in agreement with our experimental results where we observed a damping of the yield in the excitation functions between 40 and 50 MeV for the aligned configurations.

4.2. DISTRIBUTION OF THE COINCIDENCE EVENTS

Since events other than those corresponding to $\mathcal{E}_{\alpha} = 0$ are also recorded in the present experiments, their distribution in the Dalitz plot may be usefully studied with regard to assigning spins or understanding mechanisms. We develop Dalitz plot considerations here because we found that the conventionnal approaches to accounting for the coincidence events seem to fail. Four possibilities that may be considered to explain our results are given below. The fourth is an interpretation in terms of a simple, but we think meaningful, Coulomb three-body break-up of a quasi-aligned chain of the three clusters.

The coincidence results, in a three-body reaction, may be studied in the Dalitz plot by the distribution in the c.m. system of

$$\frac{d^2\sigma}{d\mathcal{E}_1 d\mathcal{E}_2} = |M|^2$$

The foregoing quantities will be plotted versus the two ^{12}C c.m. energies $\mathcal{E}_1$ and $\mathcal{E}_2$ (the label 3 is kept for the missing mass $m_3 = m_\alpha$)

The disintegration of the $^{12}C + \alpha + {}^{12}C$ system may be studied by using different simple hypotheses, which are given below:

i) statistical emission, i.e. , M = constant

ii) final state interaction in the decay of an intermediate excited fragment like , such as;

$$^{16}O^* \longrightarrow \alpha + {}^{12}C \quad \text{or} \quad {}^{24}Mg \longrightarrow {}^{12}C + {}^{12}C$$

in the two exit channels

$$^{16}O + {}^{12}C \longrightarrow {}^{12}C + {}^{16}O^* \quad \text{or} \quad \alpha + {}^{24}Mg^*$$

which lead to the same final state.

In these cases, $|M|^2$ is given a simple Breit-Wigner behaviour, depending on the width and the excitation of the intermediate level.

iii) coupling of angular momenta and correlation effects :

The simplest cases, such as giving a J value to the composite system $^{12}C + \alpha + {}^{12}C$, or a unique ℓ_i value, selected in the entrance channel, were considered. Such calculations usually refer to a particular spin value of the intermediate level. Let us call $\underset{\sim}{L_{12}}$ or $\underset{\sim}{L_{13}} = \underset{\sim}{L_{23}}$, the intermediate angular momentum ($12 \equiv {}^{12}C - {}^{12}C \equiv {}^{24}Mg^*$ and $13 \equiv 23 \equiv \alpha - {}^{12}C \equiv {}^{16}O^*$). The third particle has a residual angular momentum $\underset{\sim}{L_3}$. The coupling

$$\underset{\sim}{J} \text{ or } \underset{\sim}{l_i} = \underset{\sim}{L_{12}} + \underset{\sim}{L_3} \text{ or } \underset{\sim}{L_{13}} + \underset{\sim}{L_2}$$

involves the use of a matrix element of the type

$$M = \sum_{L_3} S^J_{L_{12},L_3} \sum_{M_{12},M_3} \langle JM_J | L_{12}L_3M_{12}M_3 \rangle \mathcal{Y}^{M_3}_{L_3}(\hat{k}_3) \mathcal{Y}^{M_{12}}_{L_{12}}(\hat{q}_{12})$$

For a real final state interaction, $S^J_{L_{12},L_3}$ is usually a Breit-Wigner term. However, the contribution of only the $\mathcal{Y}^M_L$ terms, computed with the angles defined by the experimental coincidence locus, was also estimated

The above three cases were considered as follows :

In the frame of the Lab. energies E_1, E_2, any point chosen on the coincidence locus enables us to calculate the different kinematic and geometric parameters of the three-body disintegration. The detector apertures were taken into account in the numerical transformations to estimate the matrix element M. The only effect due to the solid angles considered is an additional modulation of the distribution. This was tested in the case of the statistical emission and systematically taken into account in all our calculations.

The foregoing considerations are developed below.

4.2.1. Statistical distribution

Since M = constant, the coincidence events are expected to occur with a constant density in the Dalitz plot. A modulation due to the geometric apertures of the detectors may slightly perturb the results. However, a comparison between such theoretical predictions and the experimental results, shown in fig. 4 to 6, rules out this possibility. It may be recalled that the experimental results show that the coincidence events are predominantly characterized by two equal energies for the ^{12}C nuclei in the c.m. system; i.e., zone (a) and zone (b) defined previously).

4.2.2. Final state interaction

The coincidence plot is a powerful tool to determine the occurence of a final state interaction since there is a concentration of the events along well defined kinematic lines. For instance, in the ^{12}C - ^{12}C loci the occurence of ^{16}O or ^{24}Mg levels gives rise to concentrated events which are illustrated in Figs. 15 and 16. In

the first case, the 10.34 level was chosen in ^{16}O since it has been reported to be excited at higher incident energies [22]. This level should yield coincidence events at the intersections given by the two straight lines (shown in Fig. 15) with the three-body coincidence kinematic line. A comparison with the results of fig. 4 shows that such a sequential decay cannot explain the feeding of zones (a) and (b), as found experimentally.

^{24}Mg formation was also considered in the calculations. Since our experiment was designed to select the events which are related to very small Q energies, the feeding of a ^{24}Mg level, disintegrating subsequently into two ^{12}C's, has to occur at a very high excitation energy. For example, at 45.5 MeV, the events in zone (a) correspond to the maximum excitation of ^{24}Mg (26 MeV). However, it is shown Fig. 16 that a change of the incident energy results in a distribution of events which is not experimentally found (compare Fig. 6 with Fig. 16) Indeed, the experimental events are always in (a) or (b) whatever is the incident energy between 45 MeV and 50 MeV.

Thus the conclusion relative to these coincidence experiments is that the final state interactions like those observed in different conditions by Wieland et al[21]) or Furuno et al[22]) (^{16}O level) do not hold when the detection is sensitive to the alignment of the different momenta.

4.2.3. Correlation effects

These calculations, according to the above conclusion should be unnecessary, since no clear intermediate level seems to be found in the de-excitation process. However we tried to calculate only the effect of the $\mathcal{Y}_L^M$ terms by giving a constant value to $S^J_{L_{12},L_3}$ In such calculations, the angles $\hat{k}_3$ and $\hat{q}_{12}$ are defined relative to the beam axis which is also the quantization axis ($M_J = 0$). The choice of J, L_{12}, L_3 may be guided by the observation of the events at some particular points (zones a', b', c' defined in fig. 3). Some conclusions relative to the feeding of these areas are mentioned below.

(a) and (a') areas : their study is the motivation of the present experiments, since they correspond to $\mathcal{E}_3 = \mathcal{E}_\perp = 0$. Thus, $L_3 = 0$ and $J (= L_{12})$ is necessarily even at this point, if events are found to occur

(b) or (b') areas : in these cases, since $\hat{k}_3 = 0$ and $\mathcal{E}_3 \neq 0$, it is easy to show, according to Litherland, that M, defined in 4.2(iii), is proportional to $\mathcal{Y}^0_{L_{12}}(\hat{q}_{12})$. The study [23]) of events in such areas, versus the angle $\hat{q}_{12}$, may give L_{12}. This procedure was used at 46 MeV with coincidence results which were similar to those in Figs. 7 and 8.

(c') area : in such a case, the relative momenta k_3 and q_{12} are aligned. This means that L_{12} and L_3 are also aligned. and that $M_3 = M_{12} = M_J = 0$. Thus, M is proportional to $\mathcal{Y}^0_J(\hat{q}_{12} = \hat{k}_3)$. An application of these considerations, as well as a quantitative estimate of M, was performed chiefly for the results obtained at 46 MeV, with a view to comparing our results with those obtained in elastic scattering (the 14^+ resonance at 19.7 MeV)

Our conclusions, with regard to correlation effects, are in contradiction with the elastic scattering results, since we find that our results are better explained by an odd J value (13^- or 15^-; no events at $\xi_4 = 0$). Since our aim was not to do a correlation study, this conclusion is certainly not definitive and possible sources of contradiction will not be discussed further here.

4.2.4. Possibility of a three-body Coulomb break-up

In view of the difficulties involved in explaining our data with the usual mechanisms, we quantitatively developed another approach by taking into account the effect of the initial structure of the three clusters at the scission point and the evolution of such a system under Coulomb forces. A good knowledge of the trajectories can thus be a kind of memory of the initial configuration in the phase space, in the same way as the events related to $\xi_4 = 0$. Such an effect is expected to give a kinematic (and asymptotic) complex curve in the Dalitz plot, as do the final state interaction, by well-defined kinematic straight lines. The third dimension is then directly related to the probabilities of finding the three-body system in the configuration which is initially considered (knowledge of the wave function, as defined in 1, would be necessary). Thus, our purpose was to compute this kinematic distribution under the three-body Coulomb potentials.

The calculations were performed as described below :

At $T = T_o$ (see Fig. 1) , a judicious choice is assumed to be made for the configuration of the three clusters , defined by the relative vectors $\underset{\sim}{r}_{12}$, $\underset{\sim}{r}_{23}$, $\underset{\sim}{r}_{31}$. The three clusters $m_{1,\ 2,\ 3}$ have the momenta $\underset{\sim}{k}_{1,2,3}$

The classical laws of dynamics are employed:

i) Phase space relation

$$\sum_{ijk} \left[\mathcal{E}_i + V_{jk}(r_{jk}) \right] = \mathcal{E}_T$$

where $\mathcal{E}_i$ stands for the kinetic energy, $\left(\frac{k_i^2}{2m_i}\right)$, of mass m_i, V_{jk} is a two-body Coulomb (+ nuclear) potential between m_j and m_k and $\mathcal{E}_T$ is the available total energy due to the entrance channel: $\mathcal{E}_T = \frac{A_2}{A_1+A_2} E_o + Q$

ii) Newton's second law (3 equations)

$$\underset{\sim}{F}_i = m_i \frac{d^2 \underset{\sim}{\gamma}_i}{dt^2} = \underset{\sim}{f}_{ij}(r_{ij}) + \underset{\sim}{f}_{ik}(r_{ik})$$

$\underset{\sim}{\gamma}_i$ is the vector locating m_i relative to the three-body centre of mass ; $\underset{\sim}{f}_{ij}$'s are the two-body repulsive (+ attractive) forces deduced from the $V_{ij}(r_{ij})$ terms.

Starting from initial conditions concerning the configuration and momenta, the dynamics is expected to preserve fundamental constants such as the sum of momenta and total angular momentum J given to the system. This was checked in the evolution of the system which was computed step by step (after initial choices which will be discussed below). A set of differential equations was solved numerically. Calculations were performed in the reaction plane for each Cartesian coordinate (the centre of mass of the three clusters was

taken as the origin, the r_{12} direction was taken as X axis). In such a plane the relations ii) give rise to six one dimensional equations which, in turn, may be transformed in a set of twelve first order differential equations[24].) The system of twelve equations was solved by varying T up to T_f, such that $\sum_i \mathcal{E}_{i(T_f)} \simeq \mathcal{E}_T$. Then, two of the final three energies : $\mathcal{E}_1(T_f)$, $\mathcal{E}_2(T_f)$, are placed on the Dalitz plot. If several initial configurations are considered, the final energies, $\mathcal{E}_1$, $\mathcal{E}_2$, give rise to a "Coulomb" locus on which the events are expected if the initial conditions are good. Comparisons with coincidence experiments are then possible if the experimental locus intersects this locus. An example will be given Figs. 17 and 18.

At this stage, a discussion of the choice of initial values is necessary. The best treatment would require the knowledge of Ψ, defined in the introduction of this work, inorder to reconcile quantum and classical mechanics at the scission point. However, since the final evolution is always valid, whatever the initial conditions, some simple cases may be considered using only the two dimensional coordinates $\mathcal{E}_1$, $\mathcal{E}_2$ (the density of events, which is the third coordinate, would be given by the knowledge of Ψ).

Thus, the problem is to set the three particles in an initial configuration (aligned, quasi-aligned or triangular) such that experimental events can be accounted for.

Let us recall the relations that must hold at $T = T_o$

1) $\sum \underset{\sim}{k}_i = 0$

2) $\sum \mathcal{E}_i = \mathcal{E}_T - \sum V_{jk}(r_{jk})$

3) $\sum \underset{\sim}{k}_i \wedge \underset{\sim}{\gamma}_i = \underset{\sim}{J}\,\hbar = \sum \underset{\sim}{\ell}_i \hbar$

if 1) is used in 3) for instance, we obtain

3') $\underset{\sim}{k}_3 \wedge \underset{\sim}{r}_{23} - \underset{\sim}{k}_1 \wedge \underset{\sim}{r}_{12} = \underset{\sim}{J}\,\hbar$

with ($\underset{\sim}{r}_{23} = \underset{\sim}{\gamma}_3 - \underset{\sim}{\gamma}_2$ and $\underset{\sim}{r}_{12} = \underset{\sim}{\gamma}_2 - \underset{\sim}{\gamma}_1$)

Thus, it is obvious that some quantities in the phase space are determined by the mechanism assumed. For instance : J, $\underset{\sim}{r}_{12}$, $\underset{\sim}{k}_3$ may be chosen arbitrarily and the remaining quantities, $\underset{\sim}{r}_{23}$, $\underset{\sim}{k}_1$, $\underset{\sim}{k}_2$, are then easily deduced by solving the above equations.

What can now be said about the initial configurations mentioned above? Although Ψ is unknown a few simple cases can nevertheless be envisaged:

i) At the scission point, the total system behaves like a rigid rotor, i.e., the same angular velocity is assigned to the three clusters when they are emitted in the Coulomb fields.

ii) The entrance channel and the collision process are taken into account. For instance :

$$r_{13} = \text{constant (finite size for system } m_{13}=m_1+m_3 \equiv {}^{16}O)$$

or :
$$\underset{\sim}{v}_1=\underset{\sim}{v}_3=\underset{\sim}{v}_{\text{incident}} \text{ (break-up of } {}^{16}O \text{ at the threshold; } L_{13}=0)$$

iii) Two of the three clusters may be coupled with a fixed value of their relative angular momentum L_{ij}. This case is similar to the final state interaction, with a simple meaning. The following equation must then be added to the initial system of equations 1) to 3),

$$4) \left| \underset{\sim}{L}_{ij} \Psi \right| = \left| \frac{(m_i \underset{\sim}{p}_i - m_i \underset{\sim}{p}_i)}{m_i + m_i} \right| = \text{constant}$$

with:

$$\underset{\sim}{L}_{ij}+\underset{\sim}{L}_k = \underset{\sim}{J} = \sum \underset{\sim}{l}_i \text{ , and : } \underset{\sim}{L}_k = \frac{\sum m_i}{m_i + m_i} \underset{\sim}{l}_k ;$$

(These angular momenta, except for $\underset{\sim}{J}$, will change with the evolution of the system)

iiii) The molecular orbitals involve two relatively heavy cores and a lighter particle (alpha)

In Figs. 17 and 18 two of these cases are presented; namely i) the rigid rotor and iii), L_{ij} = constant.

With regard to the rigid rotor, it is necessary to add the two possible directions of $\underset{\sim}{J}$ relative to the planar configuration (see inset, Fig. 17, bottom left side). A symmetry $\mathcal{E}_1 = \mathcal{E}_2$ is also needed because $m_1 = m_2$. The initial configurations are then defined by:

$$\frac{J^2 k^2}{2 \sum m_i \gamma_i^2} = \mathcal{E}_T - \sum V_{ik}$$

The angular velocity and the initial momenta $\underset{\sim}{k}_i$ are then easily found, defining the initial conditions for the Coulomb trajectories. Finally, the whole Coulomb locus is computed by considering an integration of all the configurations which satisfy the above equation. In other words the finite size of the three-body system is given by this equation. The Coulomb fields due to this shape, added to the choice of the J value, define the final asymptotic locus. In Fig. 17, a case is computed with $J = \pm 14$. The initial structure is shown at the bottom of the figure.

It may be remarked that three-body Coulomb potentials are very selective. For instance, a final energy $\mathcal{E}_\infty = 0$ cannot be obtained with any configuration other than strict alignment and a critical value r_{12} (=13.8 fm) is necessary. The events which are scattered in the Dalitz plot are due to unaligned configurations. We define a degree of unalignment by the angle $\delta = (\underset{\sim}{r}_{13}, \underset{\sim}{r}_{12})$. With this definition, our experimental results correspond to linear or quasi-linear chains ($0 \leq \delta \leq 20°$).

Fig. 18 shows the computed locus when another initial condition is added (case iii), eq. 4). The results are relative to J=14 and $L_{13}=4$. The latter case concerns the ^{12}C-α coupling, in analogy with the spin value ($I=4^+$) of the 10.34 MeV state in ^{16}O. A discussion of the initial conditions can be found in ref. 25, where it is shown that, in addition to the static

configuration (given by the $\vec{r}_{ij}$ vectors) we need only to choose the angle $(\vec{k}_3, \vec{r}_{12})$ to define the three initial velocities. The closest configuration of m_3 (α), relative to m_1 (^{12}C), are shown in the lower part of the figure; they are roughly circles which are deformed in the axial region of the three aligned clusters. The relevant Coulomb locus is given in the figure. The dark areas correspond to the zones of quasi-alignment of the three clusters (heavy orbit parts). These areas are due either to a final slowing down ($\mathcal{E}_\alpha \simeq 0$), or an acceleration of the alpha by the Coulomb forces, due to the two ^{12}C, near the central region (the α velocity is approximatly tangential to the drawn orbits). For the sake of simplicity the symmetric Coulomb curve due to the identity of the ^{12}C's, has not been shown in the plot. The coupling with $L_{13}=-4$, as well as any problem of polarizability will not be discussed at the present stage.

5. CONCLUSION

Coincidence and zero angle detection methods have shown the existence of α particles emitted at rest in $^{16}O + ^{12}C$.

Such events have been considered to be the experimental signature of a ^{12}C-α-^{12}C linear chain which may be formed preferentially at some incident energies.

This study has also shown the sensitivity of the coincidence method, as well as three-body data processing, to the complex aspects of the de-excitation of the initial structure. We have tried to show that three-body Coulomb fields constitute a good memory of the initial configuration. More precisely, the events on the Dalitz plot may be scattered along some loci which are not related to the well known final-state interaction effects, but to Coulomb trajectories of the three fragments.

More generally, the present work also suggests there is a need for experimental studies at zero degrees. It would appear advisable to study some other complex systems which involve an intermediate nuclear zone between two struck nuclei. For example: high-energy central collisions (search for soft pions or any other kind of particle at zero degrees); deep inelastic collisions and ternary fission (elongated composite systems).

ACKNOWLEDGMENTS

Three of us (J.N.S., D.B., J.L.Q.) are greatly indebted to the staff of the D. Ph.N. of Saclay for the use of experimental facilities. We thank Dr J.P. Schapira for preliminary tests at zero degrees at Orsay. We are also very grateful to Messrs. Avril, Berthier, Bianchi, Chameaux and Moreau (Saclay) for help with the experiments, and we thank Messrs. Guiral and Monfouga (Bordeaux) for designing our electrostatic separator. We also thank the Tandem team of Saclay for the use of good beam transport systems. We did appreciate Dr. Mackenzie Peers's help and are grateful to him for the careful reading of this paper.

REFERENCES

1) D.A. BROMLEY, Second Int. Conf. on clustering phenomena in Nuclei, Maryland (1975)

2) Y. ABE, Int. Conf. on resonances in Heavy Ion Reactions; Hvar (1977)
T. MATSUSE, Y. KONDO and Y. ABE, RIFP 298, Kyoto Univ. (1977)

3) H. HORIUCHI, K. IKEDA and Y. SUSUKI, Sup. Progress of Theoretical Physics 52(1972)89

4) K. IKEDA and Y. SUZUKI, Second Int. Conf. on clustering phenomena in nuclei, Maryland (1975)

5) H.J. WIEBICKE, M.W. ZHUKOV, Int. Conf. on resonances in Heavy Ion Reactions, Hvar (1977)

6) -J.N. SCHEURER, N. BURNEREAU, D. BERTAULT, J.P. FOUAN J.L. QUEBERT
Second Int. Conf. on clustering phenomena in Nuclei, Maryland (1975)
-J.N. SCHEURER, J.L. QUEBERT, D. BERTAULT, J.P. FOUAN, Eur. Conf. Heavy Ions - Caen (1976) C60
-N. BURNEREAU, Thèse de 3ème cycle - Bordeaux (1975) n° 1252
-J.L. QUEBERT, J.N. SCHEURER, D. BERTAULT, J.P. FOUAN, Int. Conf. on Nucl. Structure, Tokyo (1977) 649

7) A. GOBBI, P.R. MAURENZIG, L. CHUA, R. HADSELL, P.D. PARKER, M.W. SACHS, D. SHAPIRA, R. STOCKSTAD, R.WIELAND and D.A. BROMLEY, Phys. Rev. Lett. 26 (1971) 1271

8) E.R. COSMAN, A. SPERDUTO, W.H. MOORE, T.N. CHIN and T.M. CORMIER, Phys. Rev. Lett. 27 (1971) 1074
E.R. COSMAN, A. SPERDUTO, T.M. CORMIER, T.N. CHIN, H.E. WEGNER, M.J. LEVINE, D. SCHWALM, Phys. Rev. Letters 29 (1972) 1341

9) J. GASTEBOIS, R. BALLINI, P. CHARLES, B. FERNANDEZ and J.P. FOUAN, Lettere al Nuovo Cimento 2 (1971) 90
J. GASTEBOIS, J. de Physique, Colloque C6, 32 (1971) 57

10) R. STOKSTAD, D. SHAPIRA, L. CHUA, P. PARKER, M.W. SACHS, R. WIELAND and D.A. BROMLEY, Phys. Rev. Lett. 28 (1972) 1523

11) R.E. MALMIN, R.H SIEMSSEN, D.A. SINK, and P.P. SINGH
Phys. Rev. Lett. 28 (1972) 1590

12) L.R. GREENWOOD, K. KATORI, R.E. MALMIN, T.H. BRAID, J.C. STOLTZFUS and R.H. SIEMSSEN, Phys. Rev. C6 (1972) 2112

13) B.N. NAGORCKA and J.O. NEWTON, Phys Letters 41B (1972) 34

14) P. SPERR, S. VIGDOR, Y. EISEN, W. HENNING, D.G. KOVAR, T.R. OPHEL, B. ZEIDMAN, Phys. Rev. Letters 36 (1975) 405
P. SPERR, D. EVERS, A. HARASIM, W. ASSMANN, P. KOURAD, K. RUDOLPH, G. DENHOEFFER and C. LEY, Phys. Lett. 57B (1975) 438
P. SPERR, W. HENNING and J.R. ERSKINE
Phys. Rev. C13 (1976) 447

15) D. SCHAPIRA, R.G. STOKSTAD, M.W. SACHS, A. GOBBI and D.A. BROMLEY
Phys. Rev. C12 (1975) 1907

16) M.P. WEBB, R. VANDENBOSH, K.A. EBERHARD, K.G. BERNHARDT and M.S. ZISMAN, Phys. Rev. Lett. 36 (1976) 779

17) H. FRÖHLICH, P. DÜCK, W. GALSTER, W. TREN, H. VOIT, H. WITT, W. KÜHN and S.M. LEE, Phys. Letters 64B (1976) 408

18) P. CHARLES, F. AUGER, I. BADAWY, B. BERTHIER, M. DOST, J. GASTEBOIS, B. FERNANDEZ, S.M. LEE and E. PLAGNOL, Phys. Lett. 62B (1976) 289

19) P. TARAS, G. RAO, N. SHULZ, J.P. VIVIEN, B. HAAS, J.C. MERDINGER and S. LANDSBERGER, Phys. Rev. C15 (1976) 834

20) D. SHAPIRA, R.M. DEVRIES, M.R. CLOVER, R.N. BOYD and R.N. CHERRY Jr, Phys. Letters 71B (1977) 293

21) R. WIELAND, R. STOKSTAD, A. GOBBI, D. SHAPIRA, L. CHUA, M.W. SACHS and D.A. BROMLEY, Phys. Review C9 (1974) 1474

22) K. FURUNO, K. KATORI, T. AOKI, T. OOI and J. SANADA, Int. Conf. on Nucl. Structure - Tokyo (1977) 653

23) E. FROTA DA SILVEIRA, Thèse d'Etat, Orsay (1977) n° 1825

24) TRAJEC and MERSON (CERN) codes - Bordeaux (C.E.N.B.G.) - Unpublished (1977)

25) M. CAUSSANEL, Thèse 3ème Cycle (1978); Université Bordeaux I; n° 1445

FIGURE CAPTIONS

Fig. 1 Aligned and quasi-aligned configurations 1-3-2, corresponding to the chain $^{12}C - \alpha - {}^{12}C$. Initial velocities (i.e. a J value for the system) are also considered at the initial stage of disintegration. On the right side, the qualitative evolution is considered for a large ΔT The particle is expected with zero energy for initial location at the centre of symmetry. In the other cases, the α particle may be ejected in a preferential direction depending on initial conditions. In all cases, the energies of the ^{12}C nuclei are expected to be of comparable magnitude

Fig. 2 Electrostatic deflector to detect the alpha particles emitted at zero degree. A voltage is used between (3,+30) and -(30, 3)Kvolts. The distance between the target and the counter telescope is of the order of 1.20 meter. The aperture of the collimator is 2 mm (Ø). The counter is set at 4 cm from the axis and is used to achieve the α discrimination and measure the energy. The energy acceptance is large enough in order to avoid a loss of events in the range of interest.

Fig. 3 At two given angles Ψ_1 and Ψ_2, different configurations of emission can be recorded when two particles (1,2) are detected in coincidence. The Lab energies E_1, E_2 defining an event in the cartesian plot are solutions of a relation given by the laws of conservation of momenta and energies (see 2.1).

The regions (a) and (a') correspond to $\mathcal{E}_3 = \mathcal{E}_{\alpha=0}$ events for two different values of θ. Other particular cases ($\mathcal{E}_3 \neq 0$) are shown : $\hat{k}_3 = 0$(b,b') or $\hat{k}_3 = \hat{q}_{12}$ (c').

Fig. 4 Coincidence plot obtained at 45.5 MeV for a symmetric detection ($\Theta = \pi/2$). The density of counts is given by the figures. The two curves are the limits due to the apertures of the detectors. The only events which are recorded are accumulated in zones (a) and (b) defined in Fig. 3. Despite the relative scattering for small α energies, the ^{12}C nuclei have about equal energies in the c.m system in both cases.

Fig. 5 Coincidence plot obtained at 48 MeV. The very small energies ($0 \leq \xi_\alpha \leq$ 50 kev) seem to be avoided. On average, the events occur in (a) and (b) again.

Fig. 6 Coincidence plot at 49.5 MeV. The small α energies are no longer forbidden, as they were at 48 MeV. Events are nevertheless concentrated in (b).

Fig. 7 Coincidence plot obtained at 46 MeV (about 44.5 MeV by taking into account the target thickness). The point of zero energy is indicated in the figure with the relevant configuration of emission (θ = 104°). This point is not populated ; only the spot on the right corresponds to a range of α energies of 50-200 keV. On the left side, the events correspond to 1.4 MeV $< \xi_\alpha <$ 3 MeV.

Fig. 8 Coincidence plot at 46 MeV and θ = 136°. Again, the region $\xi_\alpha = 0$ is not fed while small α energies are observed on both sides.

Fig. 9 Alpha spectra obtained at different energies with detection at zero degrees. The beam energy is given in parentheses; the average energy is given on the right after thickness corrections The spectra are normalized and the interesting energy region ($\xi_\alpha = 0 \rightarrow E_\alpha(0°) = m_\alpha A_2 Eo / (A_1 + A_2)^2$) is indicated by the arrows. A width of integration is also defined ; it corresponds to $0 \leq \xi_\alpha \leq 50$ KeV. It is worth noting the difference between the (49) and (51) MeV results.

Fig. 10 Normalized alpha spectra obtained at zero degrees and higher incident energies than those in fig. 9. Note : the strong yield of α particles emitted at rest in this region, clearly defined by a peak.

Fig. 11 Alpha spectrum obtained at 53 MeV with a QDDD spectrometer Again a clear peak is detected above the increasing background. Each point is the result of a normalization to a Rutherford scattering, used simultaneously with a gold target (1μ g/cm^2) in the reaction.

Fig. 12 Alpha energies (expected with a sequential decay) which could be intermingled with those due to the break-up of the linear chain (open circles). The detected α's are underlined and necessarily issue from the second step. The two cases to be considered are due to an α particle emitted colinearly with the other clusters ; the parent "levels" are found to be very close to the $\alpha + {}^{20}Ne$ or $\alpha + {}^{12}C$ thresholds respectively. Introduction of ${}^{20}Ne^{*}$ or ${}^{12}C^{*}$ levels results in increasing the "levels" of the same amount in energy.

Fig. 13 Total yields of coincidence events (a), (b), versus the average incident energy. The c.m. α energy corresponding to (b) is plotted at the bottom of the figure. At 45.2 MeV the (a) events have a resonant behaviour compared to (b). The lack of $\mathcal{E}_{\alpha} = 0$ events at the well known energy $\mathcal{E}$ = 19.7 MeV, should be noticed

Fig. 14 Yields of α particles with $0 \leq \mathcal{E}_{\alpha} \leq 50$ kev obtained by the coincidence method (differential cross-section) and the zero degree measurement (total cross section). The former yield is plotted with arbitrary units while the latter is estimated in absolute value. A gross structure is observed in the 22-27 MeV region of ${}^{28}Si$. A fine structure is more difficult to show.

Fig. 15 Simulation of a final state interaction on the coincidence plot. An ${}^{16}O$ level is considered at 10.34 MeV (4+). The result is to be compared to the experimental plot of Fig. 4, obtained at 45.5 MeV. It is easy to check that such a crossing is unable to account for the results obtained in (a) and (b), even if the level value or the incident energy is changed.

Fig. 16 Simulation of a ${}^{24}Mg$ "level" (26 MeV). This choice is revealed to be inadequate when the incident energy is changed, since the relevant events are moved in between the two regions (a, b) where no events occur.

Fig. 17 Different representations of the ^{12}C c.m. energies ε_1 , ε_2 in the three-body disintegration $^{12}C + \alpha + ^{12}C$. The Dalitz limit is given by (1). The coincidence experiment at 45.5 MeV ($\vartheta_1 = \vartheta_2 = 36.7°$) defines a kinematic distribution given by (2) on whi ch the recorded data (already shown in the Lab. system in fig. 4) are indicated by the dashed areas (left side) . The rigid body equation : $\frac{J^2 \hbar^2}{2 \sum m_i r_i^2} = \varepsilon_T - \sum V_{ik}$ leads to the elongated three-body configuration shown at the bottom of the figure. Any location of the alpha particle is considered and the relevant Coulomb break-up gives rise to curve (3) when two opposite rotations $J=14^{(+)}$ and $J=14^{(-)}$ are considered. On such a complex locus (3) the parts due to small disalignments of the chain ($0 \leq \delta \leq 20°$) are given by the heavy lines; they correspond roughly to our experimental observation , with a discrepency near $\varepsilon_\alpha = 0$, easy to explain by the simplicity of the assumption.

Fig. 18 The asymptotic ^{12}C energies represented as in Fig. 17, when a relative coupling $L_{13} = 4$ is used to define the initial conditions . The closest locations of the alpha particle are shown at the bottom of the figure. These "orbits" are chiefly deformed from a circle in the axial region. The relevant Coulomb locus (3) is also shown when the alpha location is changed. The dark areas correspond to initial locations close to alignment. The alpha initial velocity is roughly tangent to the drawn orbits.

T_0	$T_0 + \Delta T$
①③② $J_{PLANE}=0$ { NO INITIAL VELOCITIES	① ③ ② $\varepsilon_3 = 0$ $\varepsilon_1 = \varepsilon_2 = \varepsilon_T/2$
①③② $J_{PLANE}=0$ { NO INITIAL VELOCITIES	③ ① ≃90° ② $\varepsilon_3 \neq 0$ $\varepsilon_1 \simeq \varepsilon_2 < \varepsilon_T/2$
①③② $J_{PLANE}\neq 0$ { INITIAL VELOCITIES FOR 1, 2	② ③ ① $\varepsilon_3=0$ $L_3=0$ $\varepsilon_1 = \varepsilon_2$ $L_{12}\neq 0$
①③② $J_{PLANE}\neq 0$ { INITIAL VELOCITIES FOR 1, 2, 3	③ ① ② $\varepsilon_3 \neq 0$ $L_3 \neq 0$ $\varepsilon_1 \simeq \varepsilon_2$ $L_{12}\neq 0$

Fig 1

Scheuer et al

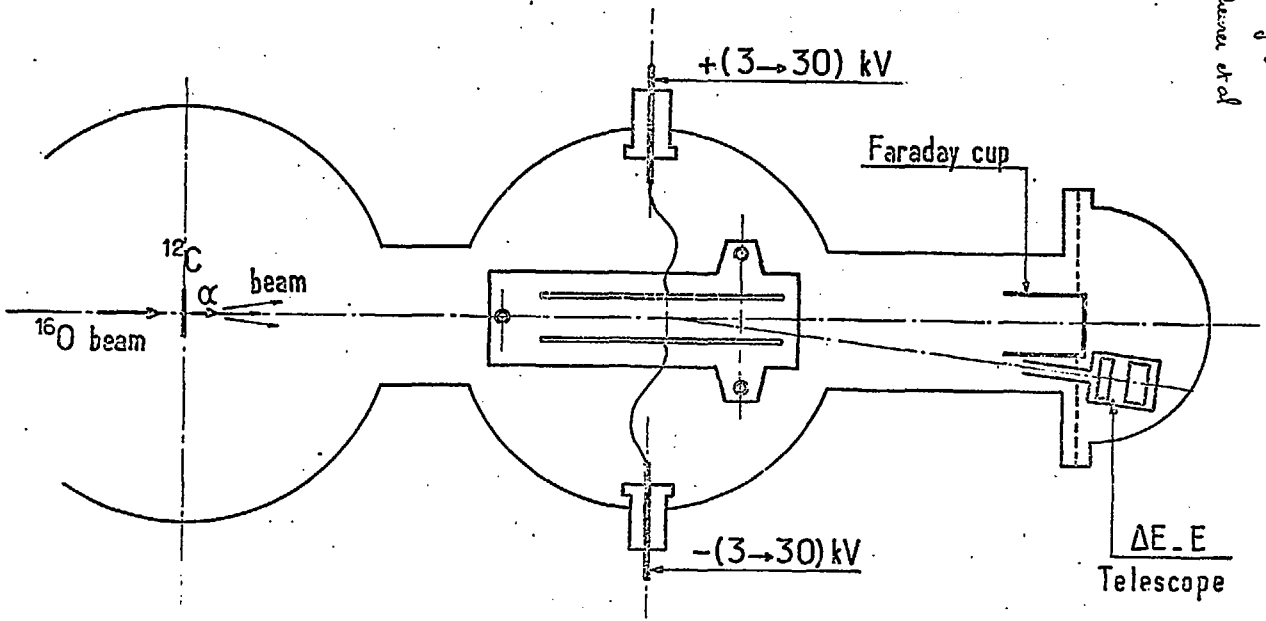

Fig 2
Schewer et al

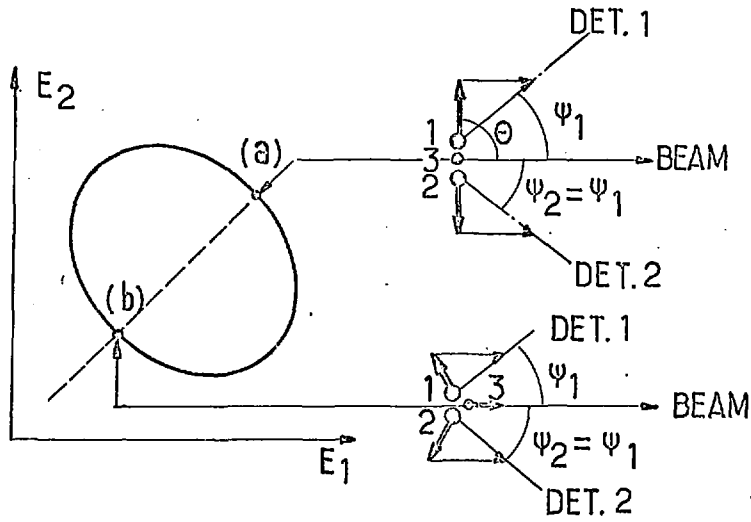

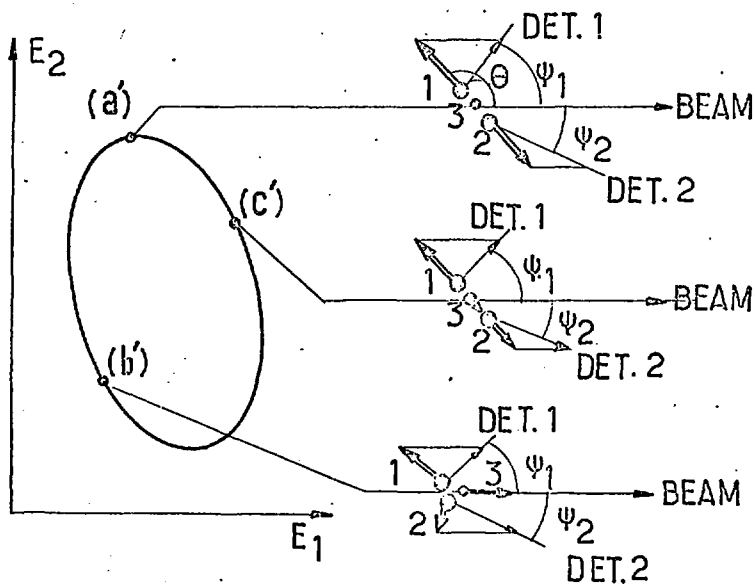

Fig. 3

Schaner et al

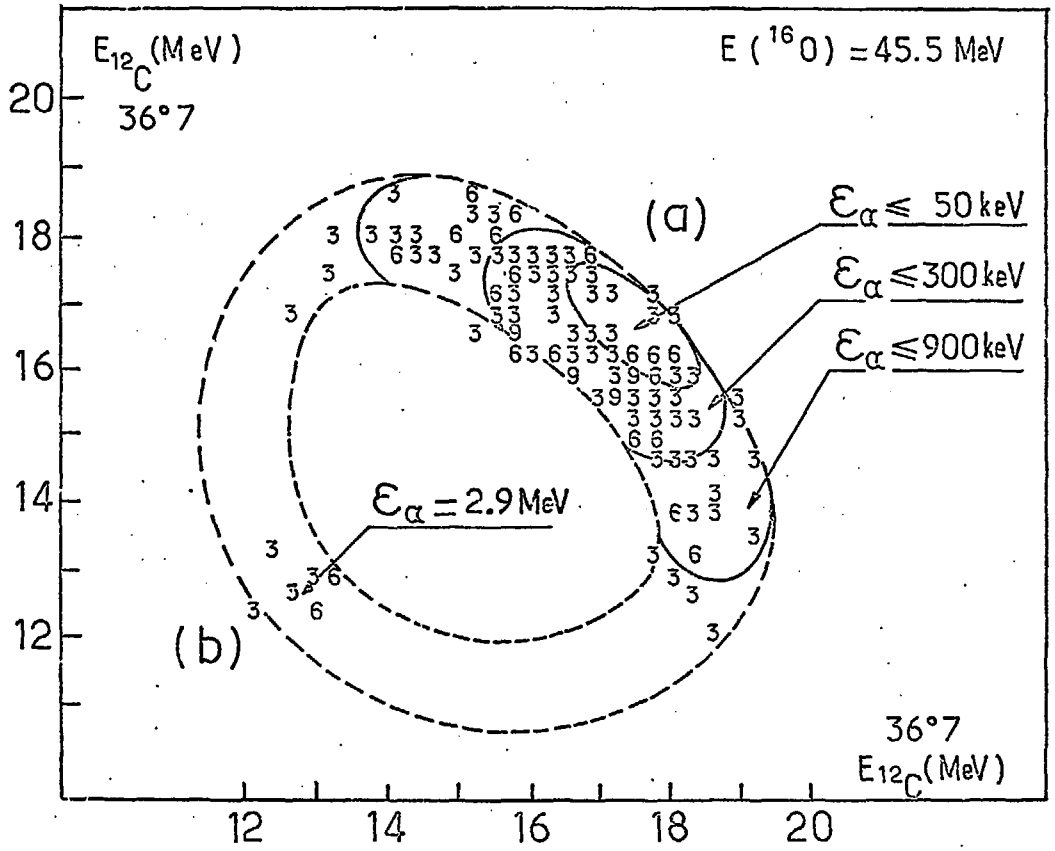

Fig. 4
Schwarz et al.

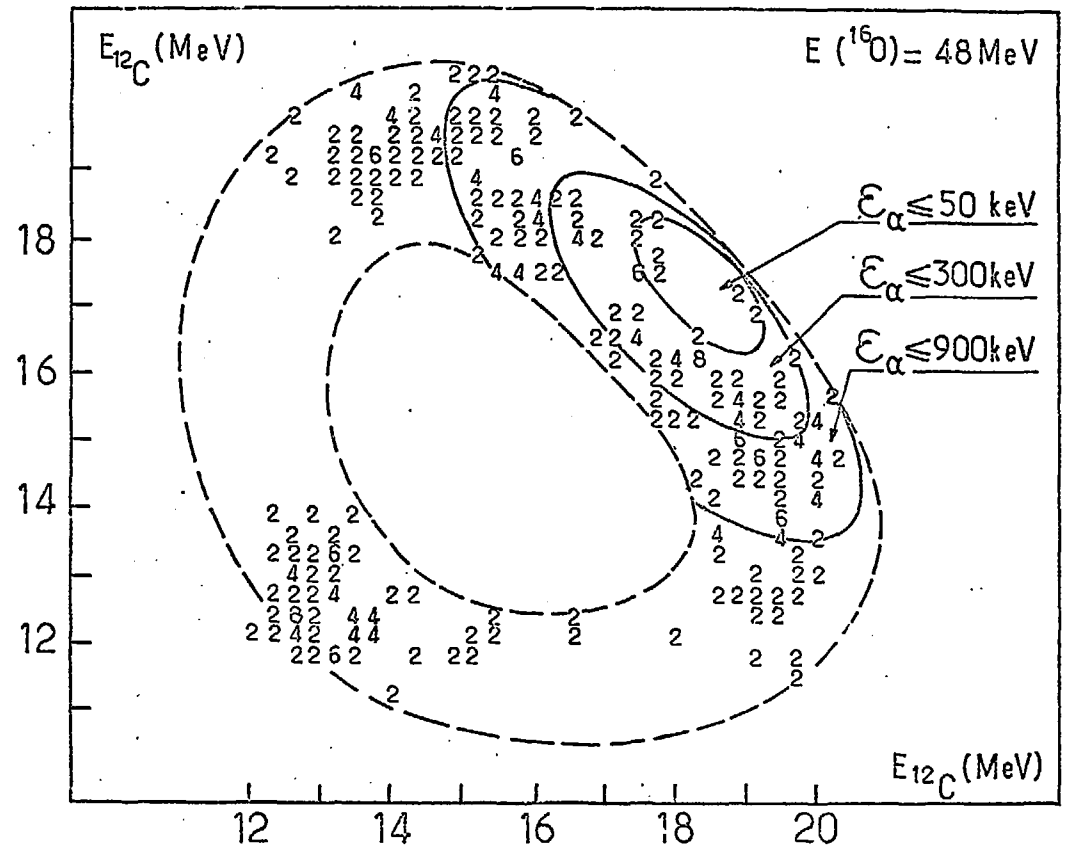

Fig 5
Schwarz et al

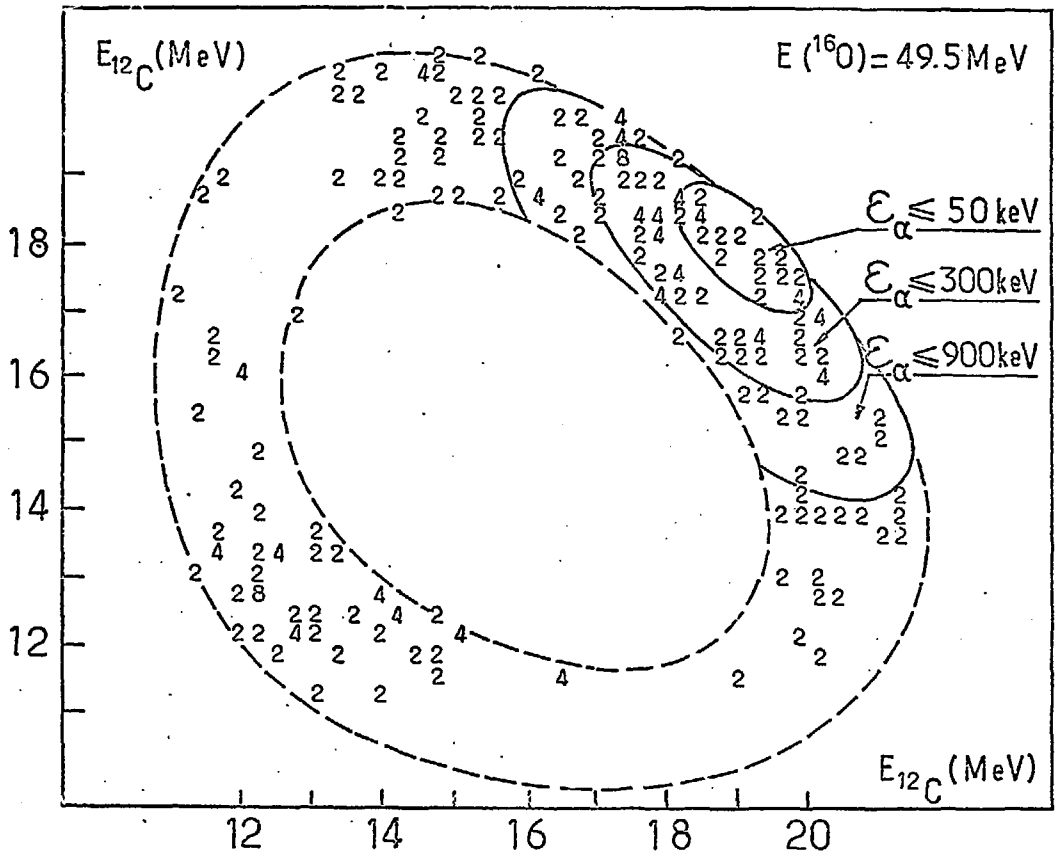

Fig 9

Schwarz et al

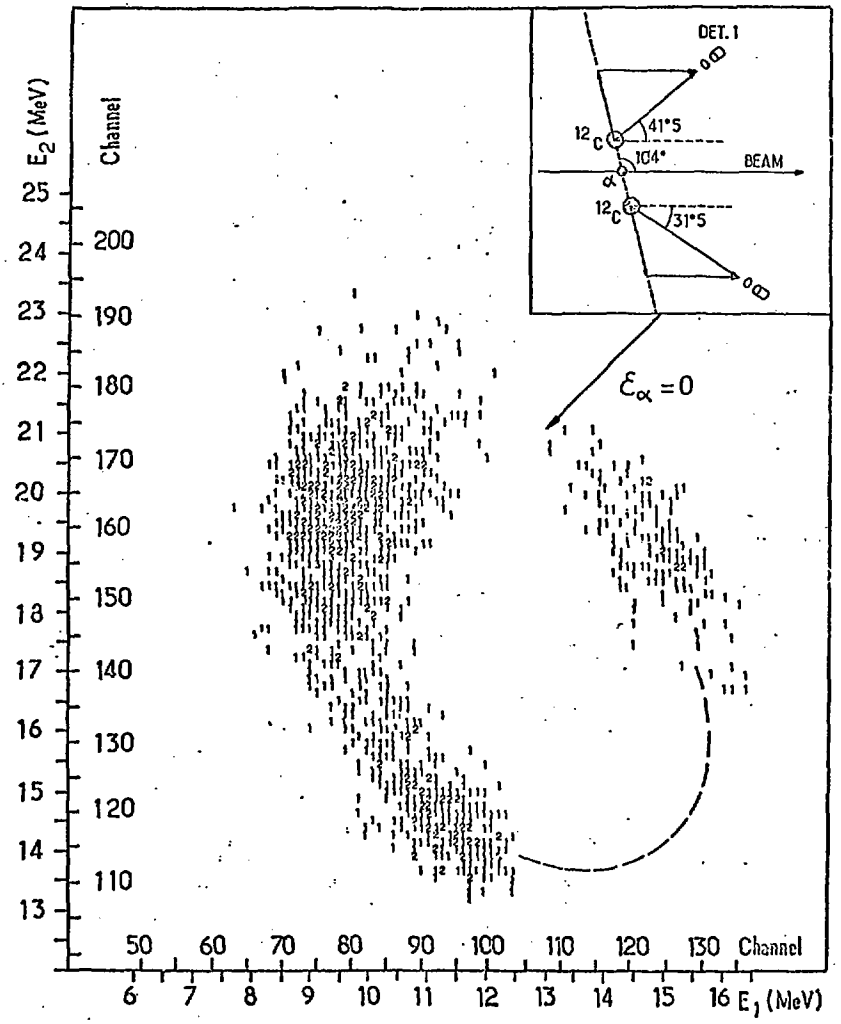

Fig 7

Scheuer et al

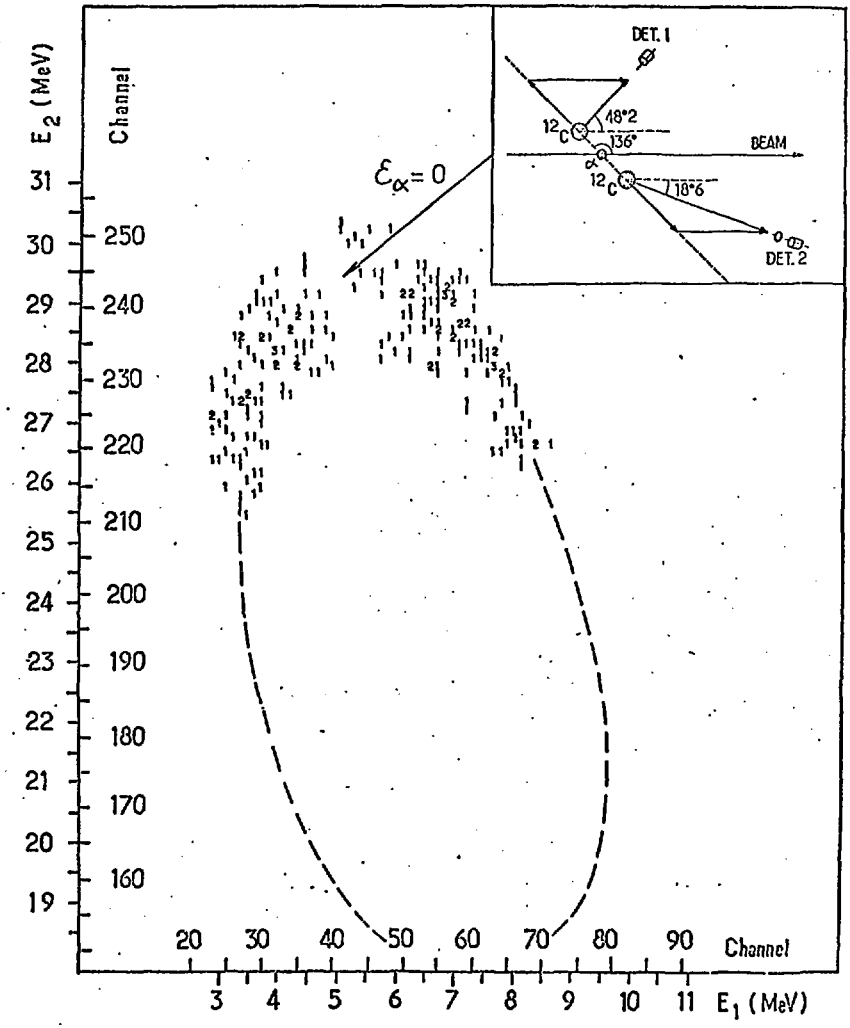

Fig 8

Scheuer et al

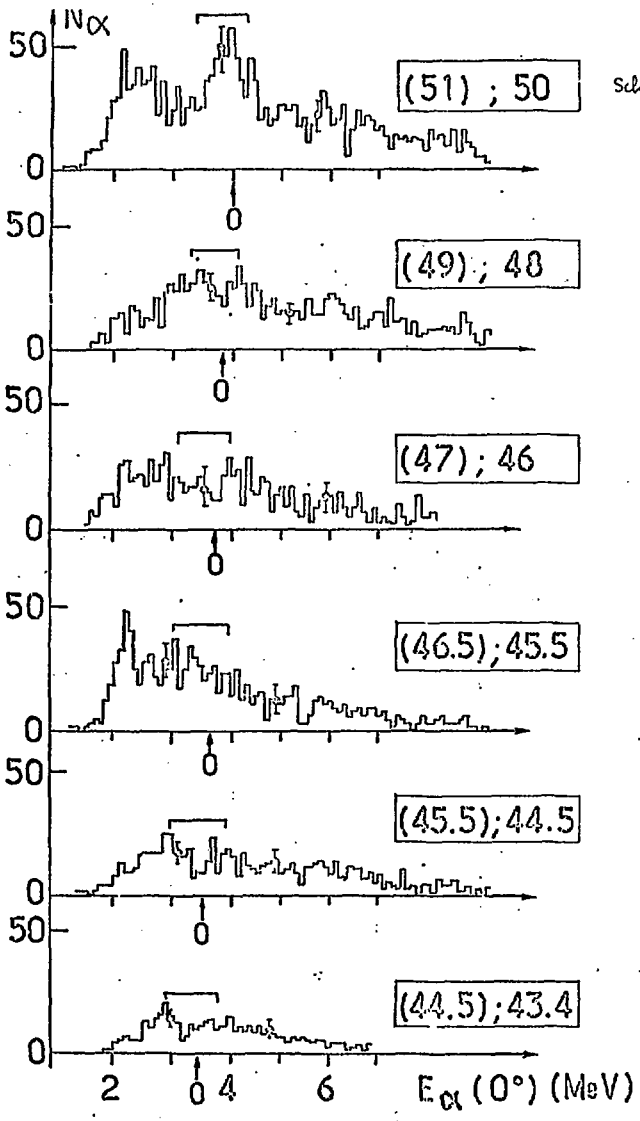

Fig 9
Scheurer et al

Fig 10
Scheuer et al

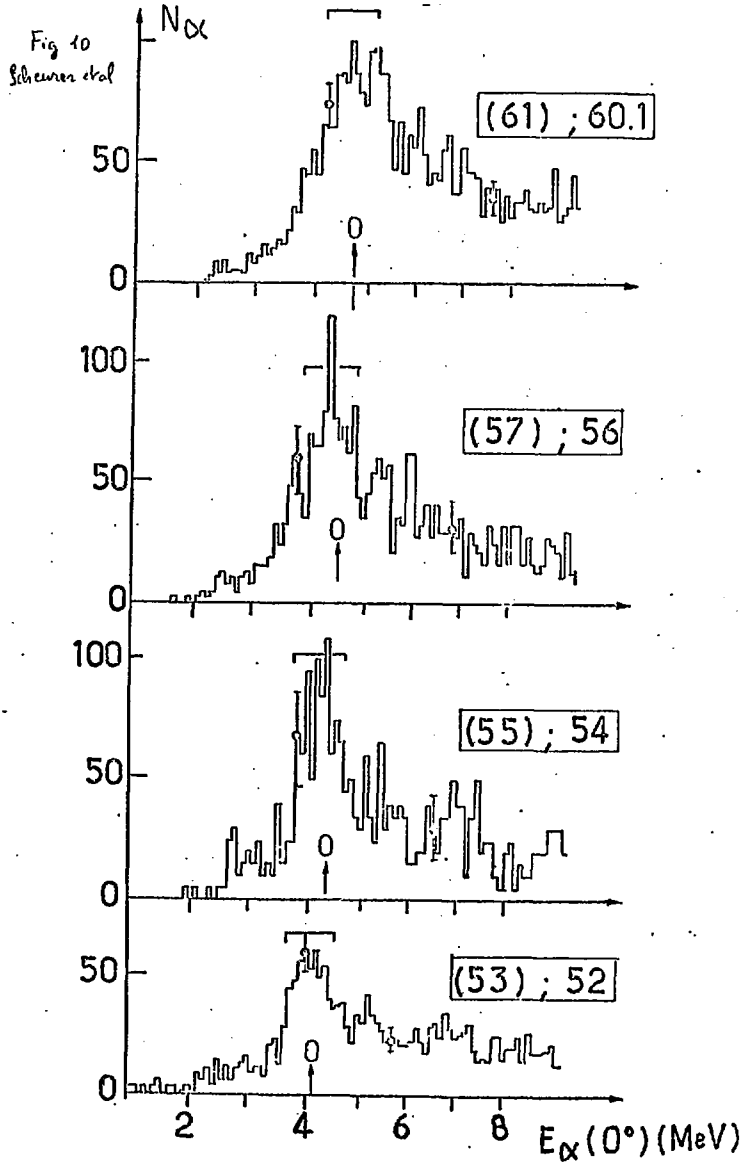

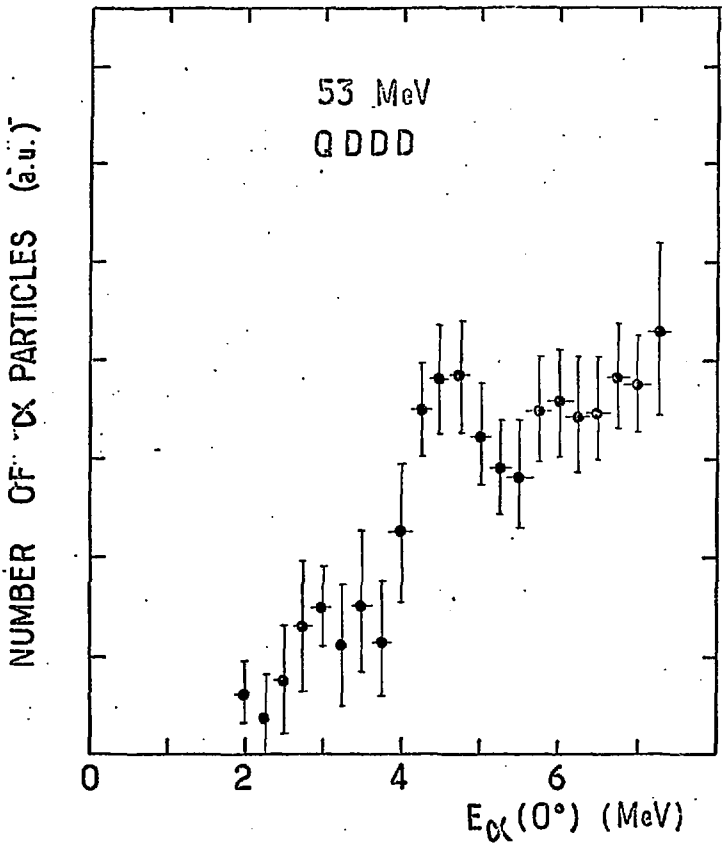

Fig 11
Scheuer et al

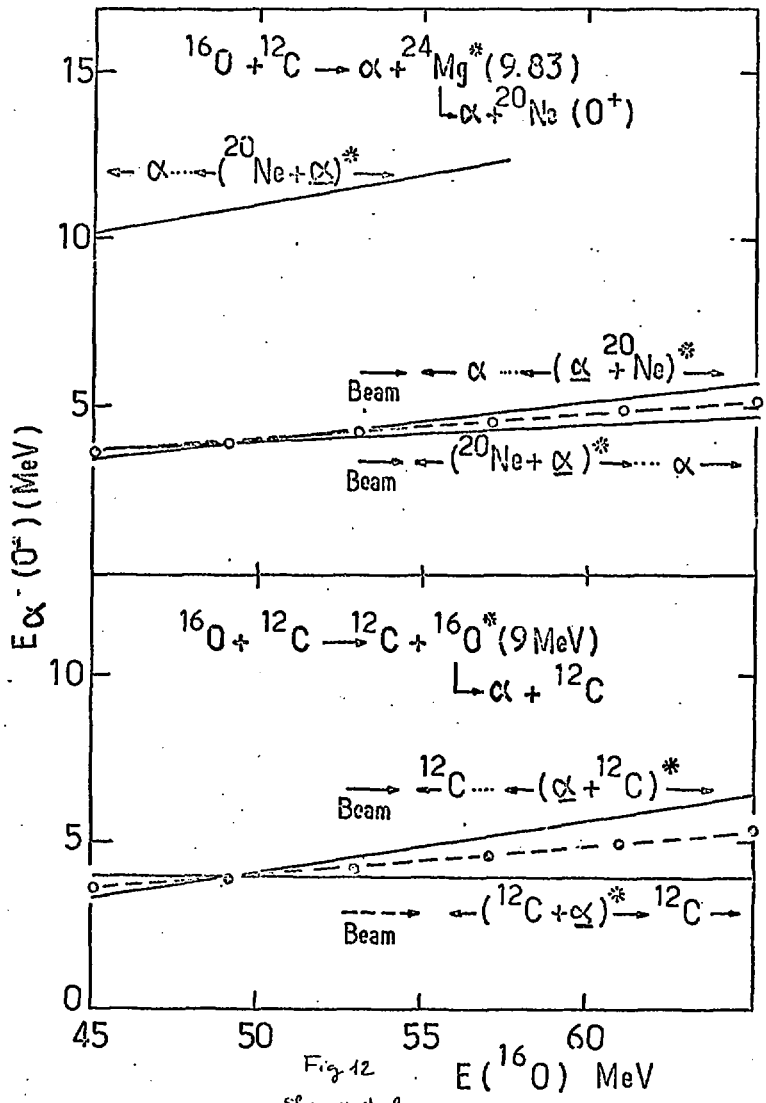

Fig 12

Shearer dral

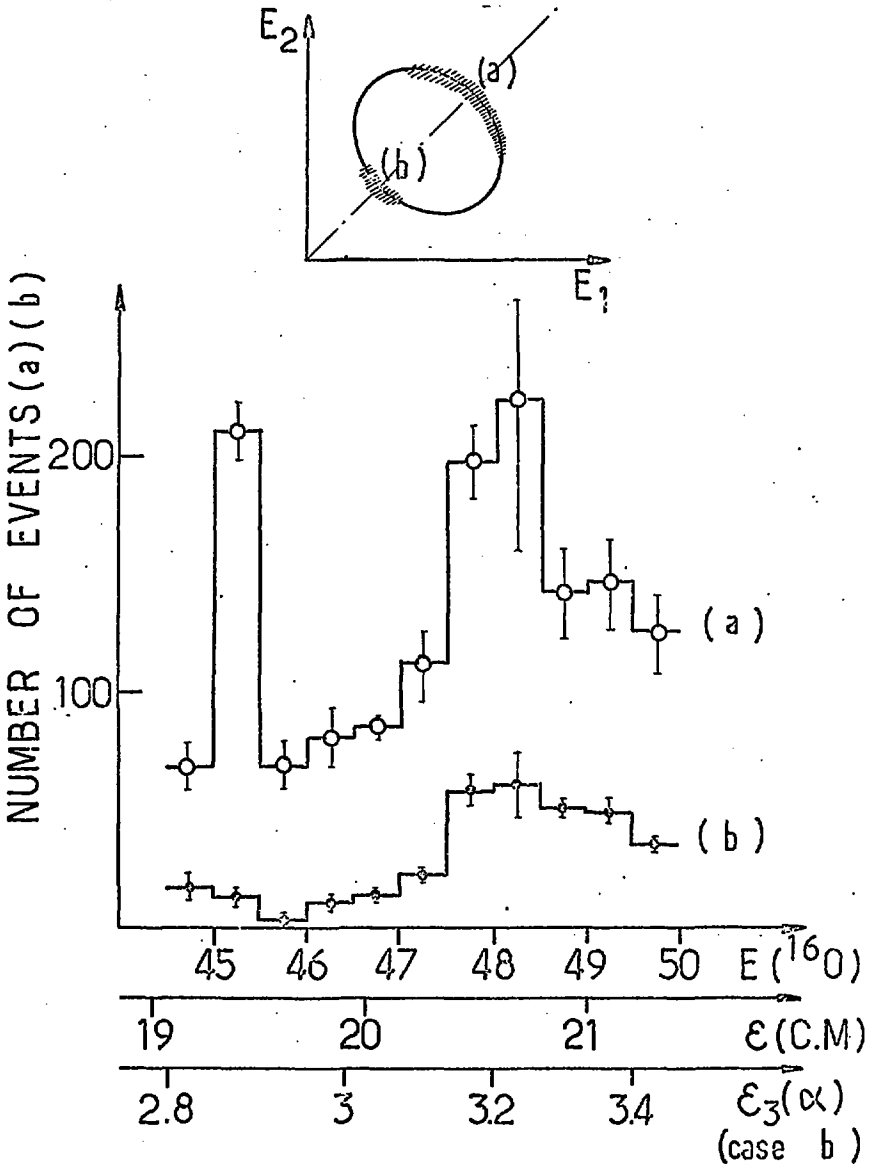

Fig 13

Scheuer et al

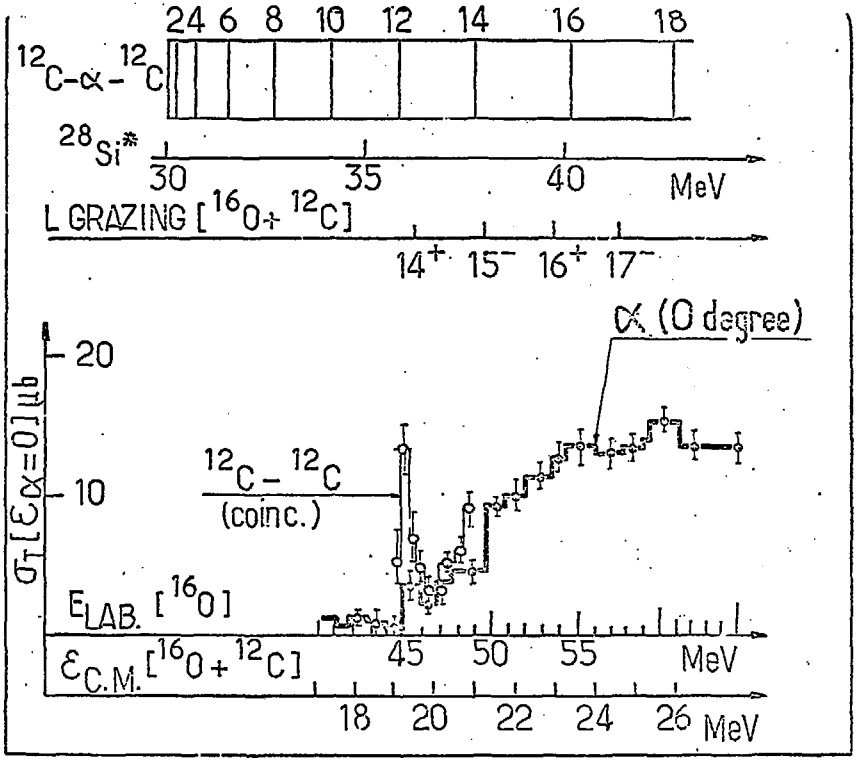

Fig. 14
Schwarz, Ref.

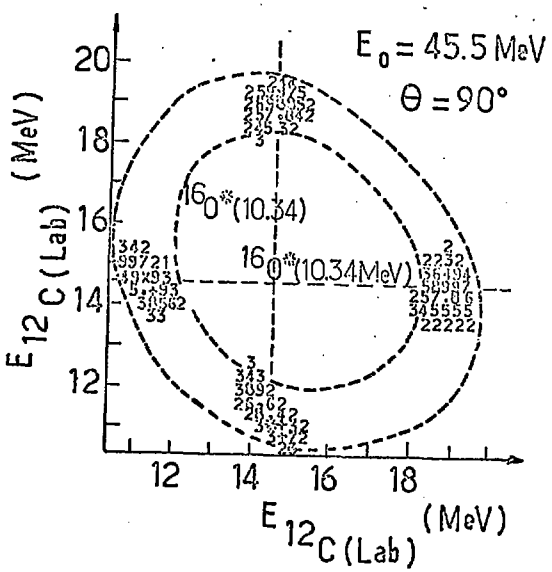

Fig 15
Scheurer et al

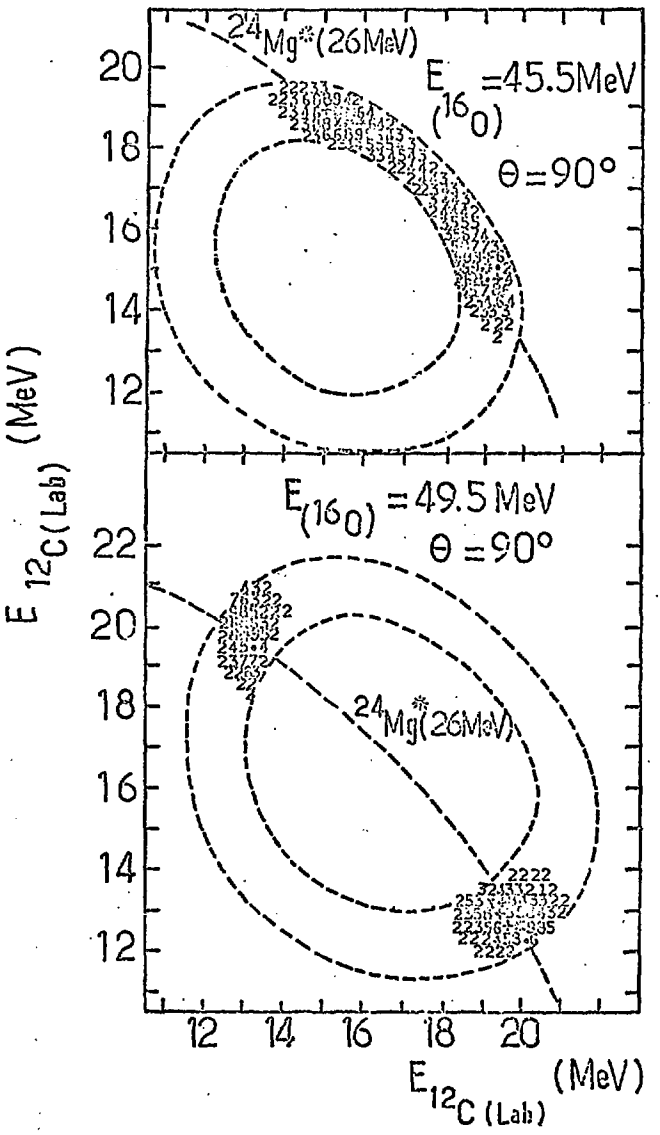

Fig 16

schema eval

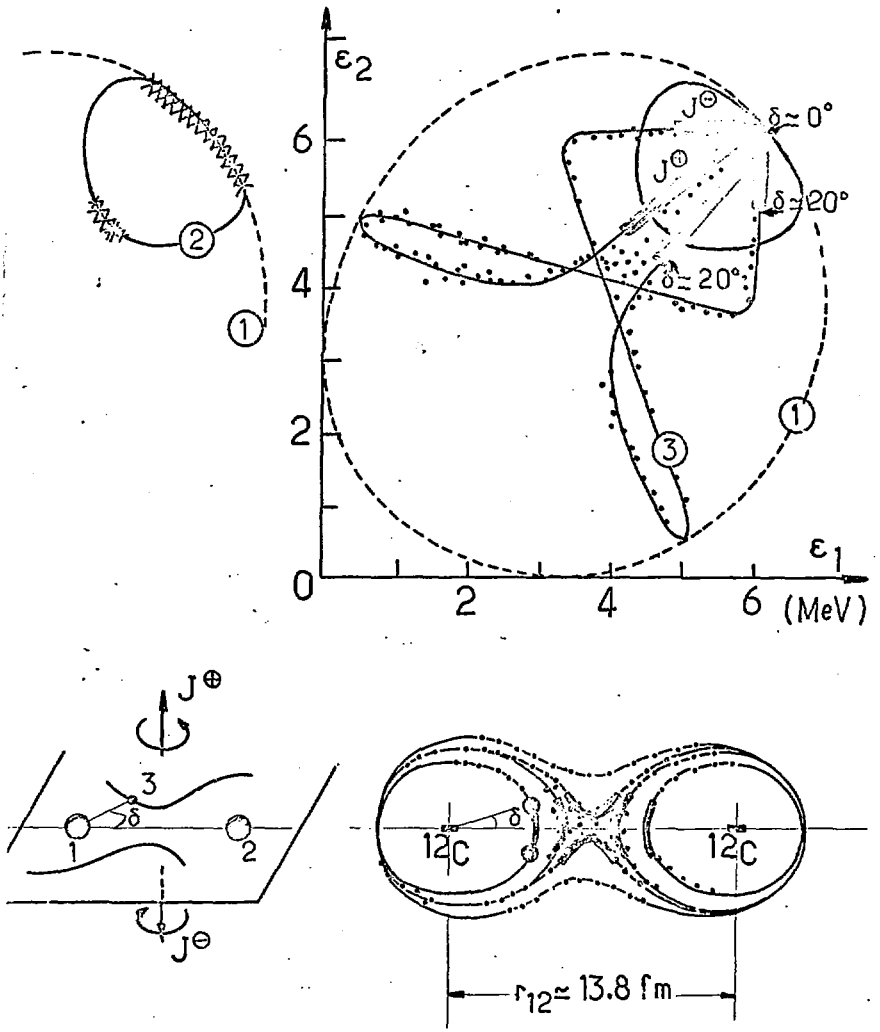

$E_{INC} = 45.5$ MeV ; $J = 14$

Fig. 17
Scheurer et al

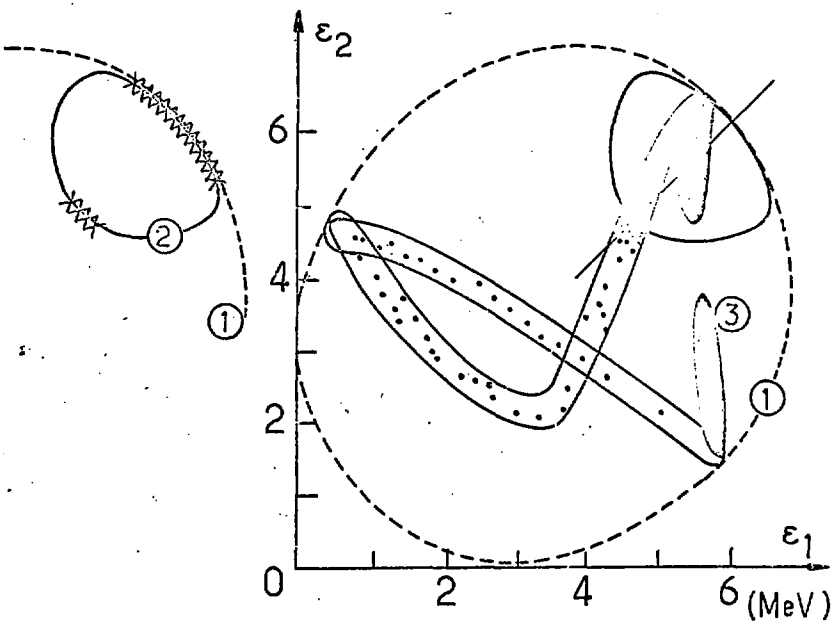

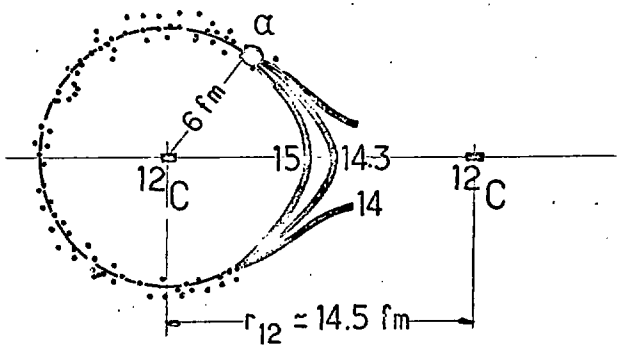

$E_{INC} = 45.5\,MeV\,;\ J = 14\ ;\ L_{13} = 4$

Fig 18
Schemes of reaction